Int J Pept Res Ther
DOI 10.1007/s10989-010-9211-2

Conformational Analysis of a Synthetic Antimicrobial Peptide in Water and Membrane-Mimicking Solvents: A Molecular Dynamics Simulation Study

Sandro L. Fornili · Rita Pizzi · Davide Rebeccani

Accepted: 23 April 2010

Abstract We have investigated structural and dynamic properties of the synthetic peptide hlF1-11 (GRRRSV QWCA, i.e., the first 11 N-terminal amino acids of the human lactoferrin protein) in water, 250 mM NaCl solution, 50% (V/V) water–trifluoroethanol mixture, and in the membrane mimetic 4:4:1 methanol–chloroform–water mixture. For comparison, we have also performed analogous simulations for the biologically inactive control peptide featuring Ala substitutions in the 2, 3, 6 and 9 positions of the hlF1-11 sequence. Statistical analyses of the trajectories indicate that only in the membrane-mimicking medium hlF1-11 adopts preferentially a conformation suitable to interact effectively with the membrane. In this conformation the peptide cationic region is rather flexible and elongated, while the C-terminal hydrophobic moiety appears as a more rigid hairpin-shaped loop approximately perpendicular to the cationic region. No such conformation is statistically relevant for the control peptide.

Keywords Antimicrobial peptides · Human lactoferrin · Molecular dynamics simulation · Membrane-mimicking solvents

S. L. Fornili (✉) · R. Pizzi · D. Rebeccani
Dipartimento di Tecnologie dell'Informazione, Università di Milano, Via Bramante 65, 26013 Crema, Italy
e-mail: sandro.fornili@unimi.it

S. L. Fornili
CISI, Via Fantoli 16/15, 20138 Milan, Italy

S. L. Fornili
CNISM, Via della Vasca Navale 84, 00146 Rome, Italy

Introduction

The broad range of effectiveness of cationic antimicrobial peptides (AMPs) is thought to be mainly due to their often disruptive interaction with the cellular membranes of bacteria, fungi and viruses (Brogden 2005; Chan et al. 2006; Yeaman and Yount 2003). The characteristics of such interaction are related to structural properties of peptides (Powers and Hancock 2003). They can be investigated using experimental CD and NMR techniques as well as statistical mechanical simulations (Langham et al. 2008), which provide atomic-level details of the system behavior.

In the present work we report results of Molecular Dynamics (MD) simulations of solutions of the cationic AMP hlF1-11 (GRRRRSVQWCA) (Nibbering et al. 2001; Dijkshoorn et al. 2004) in various solvents, in order to enlighten its structural and dynamic properties in environments suitable to the experimental research, thus favoring their comparison with experimental structural data. The latter are presently not available to the best of our knowledge for hlF1-11. The interest for the synthetic hlF1-11 peptide, which consists of the first eleven N-terminal amino acids of the first cationic domain of the human lactoferrin protein, stems from its broad antimicrobial activity against bacteria and fungi, and in particular against bacterial strains resistant to conventional antibiotics (Nibbering et al. 2001; Dijkshoorn et al. 2004). We have also simulated a biologically inactive control peptide (GAARRAVQACA, that is the hlF1-11 sequence with Ala substitutions at positions 2, 3, 6 and 9) (Brouwer and Welling 2008).

Since solvent affects the peptide 3D structure (Ruotolo and Russell 2004), in order to get some insight into the interaction mechanisms between AMPs and bacterial

Published online: 22 May 2010

membranes it is important to investigate which conformations they most probably adopt in environments similar to that of cellular membranes (Haney et al. 2009). Therefore, besides simulating both peptides in water, we also carried out simulations in the following media: (i) 250 mM aqueous solution of NaCl (referred to as "salt" medium in what follows), since salt has been shown to stabilize marginally stable peptide structures (Ibragimova and Wade 1998; Zhou et al. 2004); (ii) 4:4:1 methanol–chloroform–water mixture (called "441" medium in the following), an isotropic solvent mimicking the anisotropic cell membrane environment (Mottamal et al. 2007); (iii) 50% (V/V) water–trifluoroethanol (TFE) mixture, recently used in an experimental work as mimicking the membrane environment (Wang et al. 2008).

Statistical analyses of extensive simulations of both peptides in these media show that hlF1-11 (but not the control peptide) in 441 adopts preferentially a conformation in which the rather linear and flexible cationic N-terminal region and the hairpin-shaped and more rigid hydrophobic C-terminal moiety are spatially well distinct and approximately mutually perpendicular. Moreover, the probability of finding chloroform molecules around the latter region is higher than around the peptide cationic part, while the opposite occurs for water and methanol molecules. All this would suggest that hlF1-11 behaves as a loop-type AMP (Powers and Hancock 2003) while interacting with the bacterial membrane.

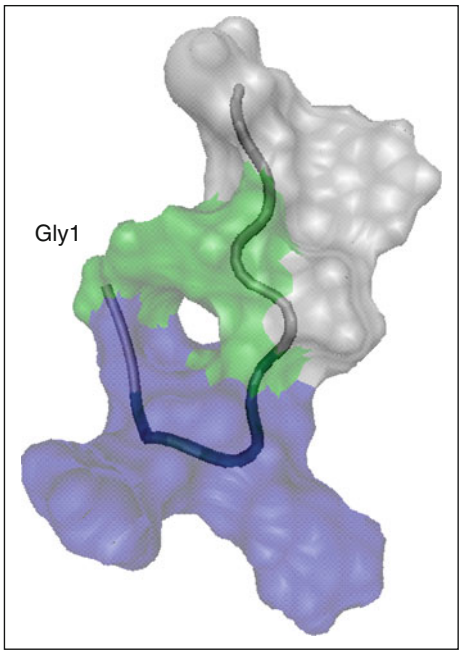

Fig. 1 Initial hlF1-11 conformation taken from the PDB code 1h45 (Peterson et al. 2002), except for Gly1 and Arg2, whose coordinates were missing. Surface and backbone colors are set according to the VMD color-coding. Surface colors corresponding to polar, non-polar and basic residues are *green*, *white* and *blue*, respectively (Color figure online)

Computational Methods

Each simulation was carried out for 100 ns at $T = 300$ K, $P = 1$ bar and 2-fs time step, using the all-atom ff99SB force field (Wickstrom et al. 2009) and the SANDER module of the AMBER10 package (Case et al. 2005, 2008). Temperature was controlled according to the Berendsen coupling algorithm (Allen and Tildesley 1987) with 1-ps time constant, while the time constant of the pressure control was 2.5 ps. A 9-Å cut-off value and particle mesh Ewald (PME) were adopted for the nonbonded interactions. SHAKE (Allen and Tildesley 1987) kept constrained bonds involving hydrogen atoms. The initial coordinates of the hlF1-11 peptide were taken from the N-terminal lobe of the human lactoferrin (PDB code 1h45 (Peterson et al. 2002), Fig. 1). The coordinates of two N-terminal amino acids missing in this PBD file were added using the AMBER10 xLEaP module, which was also used to build up the initial conformation of the control peptide, to neutralize the peptide charges with counterions, and to add an equal number of Na^+ and Cl^- ions for the "salt" solvent. The initial conformations of both peptides were used as input for 50-ns implicit-water–solvent MD simulations performed according to the Generalized Born model as implemented in AMBER10 (Onufriev et al. 2004). Cluster analysis was applied to the resulting trajectories. For each peptide, the conformation representative of the most populated cluster was adopted as initial conformation for all the explicit-solvent simulations using the solvents mentioned in the previous section. Each simulated system (Table 1) included one peptide immersed in a truncated octahedron solvent box with a minimum distance of at least 10 Å between peptide atoms and box surface. The solvent models were TIP3P water (Jorgensen et al. 1983), methanol (Caldwell and Kollman 1995), chloroform (Fox and Kollman 1998) and TFE (Abbate et al. 2006). Most of the statistical analyses of the trajectories have been performed using the AMBER 10 PTRAJ module. Voronoi volume and Solvent Accessible Surface Areas (SASA) values were calculated as outlined in (Voss and Gerstein 2005). Graphical visualization was performed with VMD (Humphrey et al. 1996) and gOpenMOL (Bergman et al. 1997).

Results and Discussion

The upper and the lower rows of Fig. 2 show the time evolution of the backbone RMSD and gyration radius, respectively, for hlF1-11 (left column) and control peptide (right column) during 100-ns explicit-solvent MD simulations in water, 250 mM salt solution, and in the 441 and

Table 1 Composition of the simulated systems

	Water	Salt	441	Water–TFE
1 hlF1-11 + $4Cl^-$	2500w	2506w + 15NaCl	1012m + 1012c + 253w	366w + 508t
1 control + $2Cl^-$	2501w	2503w + 15NaCl	1003m + 1004c + 251w	366w + 508t

The labels salt, 441, and water–TFE indicate 250 mM NaCl solution, 4:4:1 methanol–chloroform–water mixture, and 50% (V/V) water–TFE mixture, respectively; w, m, c and t represent water, methanol, chloroform and TFE molecules, respectively

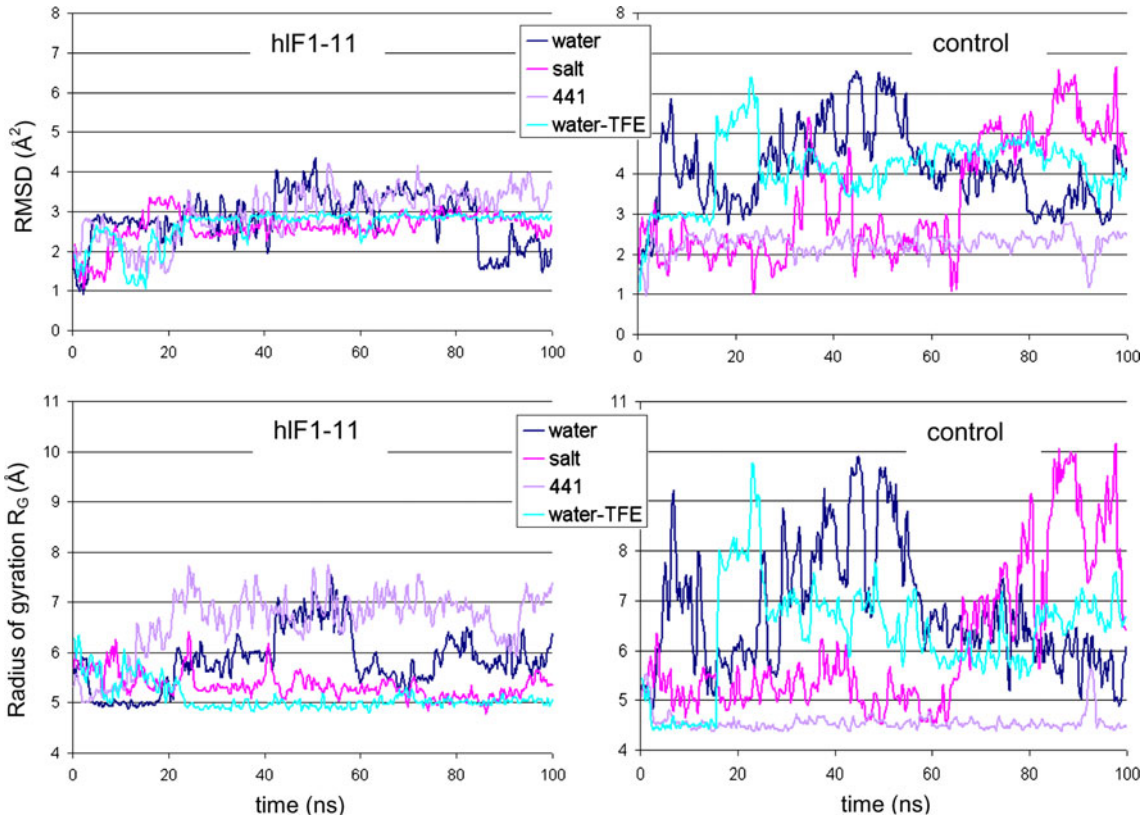

Fig. 2 Backbone RMSD (in $Å^2$, *upper row*) and radius of gyration, R_G, (in Å, *lower row*) versus time (in ns). *Left column*: hlF1-11; *right column*: control peptide

water–TFE membrane-mimicking mixtures. The reference structures for RMSD calculations were taken from the last conformations of the equilibration phase.

The RMSD evolution evidences that in general the conformational variability is lower for hlF1-11 than for the control peptide. It is also worth noting that in salt and in water-TFE the values of the hlF1-11 gyration radius are particularly small and almost constant, suggesting that the peptide backbone conformation in these solvents is more compact than in water and in 441. This observation agrees with the average values of the gyration radius reported in Table 2, which have been calculated over the 50–100 ns time intervals of the trajectories.

The additional statistical analyses, whose results are discussed in the following, have been performed considering the same time interval. In particular, in Table 2 we report values of the Solvent Accessible Surface Area (SASA) as probed by the water molecule (i.e., using 1.4-Å probe radius), and of the molecular volume, which has been calculated according to the Voronoi procedure. As expected, both these quantities are smaller for the control peptide than for hlF-11, due to the above mentioned Ala substitutions. Moreover, on can observe that the Voronoi volumes slightly decrease passing from water to salt, 441 and water–TFE solvents. Positive SASA differences occur only for hlF1-11 in 441 and for the control peptide in salt. It is perhaps worth noting that only for these solvents positive variations of R_G occur. Data shown in Table 2 could also be of interest while comparing simulation and experimental structures, or even to predict peptide biological properties using them in QSARs as in Langham et al. 2008.

Table 2 Structural data for hlF1-11 and control peptides

	Water	Salt	441	Water–TFE
hlF1-11				
R_G (Å)	6.0 (0.0)	5.2 (−13.3)	6.9 (15.0)	6.0 (0.0)
SASA (Å^2)	1531.8 (0.0)	1478.6 (−3.5)	1616.7 (5.5)	1391.4 (−9.2)
VorVol (Å^3)	1770.1 (0.0)	1776.9 (−0.1)	1720.6 (−3.3)	1674.4 (−5.9)
Control				
R_G (Å)	6.5 (0.0)	6.9 (5.8)	4.6 (−41.3)	6.3 (−3.2)
SASA (Å^2)	1308.1 (0.0)	1383.8 (5.8)	1138.6 (−13.0)	1269.0 (−3.0)
VorVol (Å^3)	1419.1 (0.0)	1423.0 (0.3)	1344.2 (−5.3)	1332.8 (−6.1)

Percentage differences with respect to values in water are reported in parentheses. R_G radius of gyration, *SASA* solvent accessible surface area using 1.4-Å probe radius, *VorVol* Voronoi volume

In Fig. 3 we report statistically representative conformations of the most populated clusters as obtained by applying to hlF1-11 trajectories the average-linkage clustering procedure, which is likely one of the best performing clustering algorithms and particularly suited to bioinformatic issues (Shao et al. 2007). Analogous results for the control peptide are shown in Fig. 4. In agreement with the above observations concerning the gyration radius, we see from Fig. 3 that the most compact hlF1-11 conformation occurs in salt, and the most extended one in 441 medium, where the spatial separation between the cationic and the hydrophobic moieties of the peptide is most pronounced. It is worth noting that this conformation could favor the peptide interaction with bacterial membrane since the well exposed cationic domain could be attracted by the anionic heads of the membrane while the loop-shaped hydrophobic domain, which forms with the cationic moiety an angle of approximately 90°, could interact with the membrane hydrophobic interior (Brogden 2005). According to this view hlF1-11 could be assigned to the class of loop-AMPs (Powers and Hancock 2003).

A further observation concerning Fig. 3 is that the hlF1-11 statistically most representative conformations in 441 and water–TFE mixtures are quite different, although these solvents are both assumed to be reasonably good mimetics of the membrane environment. Finally, we note that none of hlF1-11 conformations reported in Fig. 3 resembles its initial conformation (Fig. 1), whose experimental coordinates were taken from Peterson et al. 2002 except for those of Gly1 and Arg2 residues.

In Fig. 4 we report analogous results concerning the control peptide, whose amino acid sequence is the same as that of hlF1-11 but with Ala substitutions in positions 2, 3, 6 and 9, as above pointed out. Due to these substitutions, its cationic and hydrophobic moieties are not clearly distinct as in hlF1-11 peptide. Also for the control peptide, however, the overall aspects of the representative conformations of the most populated clusters agree with the above considerations concerning the radius of gyration behavior in different solvents. In particular, the most compact conformation occurs in the 441 mixture (Table 2) and it corresponds to a partial α-helical structure involving the residues from Ala2 to Ala6. From Fig. 4 one can also observe that in none of the chosen solvents the statistically predominant conformations of the control peptide are elongated as that of hlF1-11 in 441 medium.

The molecular structures shown in Figs. 3 and 4 can be correlated with the results of hydrogen bond (HB) analysis reported in Table 3, where we report the most relevant HBs, the percentage of snapshots in which they are present along the 50–100 ns interval of the pertinent trajectories, and the average frequency of all HBs with frequency larger than 5%. An overall view of these data shows that in general the hydrogen bonding is more relevant for hlF1-11 than for the control peptide, except than in 441 solvent, where the structure of the control peptide is partially helical, as previously mentioned. One can also observe that the β-turns present on the most representative hlF1-11 conformations in water and water–TFE solutions are mostly stabilized by the presence of the HB between Arg4 and Val7 amino acids, while the most persistent HB between Cys9 and Arg3 β-bridges is related to the rather closed structure adopted by hlF1-11 in the salt medium, and the HB between Val7 and Cys10 is connected to the looping-back structure of the hlF1-11 hydrophobic moiety in the 441 solvent.

Examining the most persistent HB of the control peptide we can see that Gln8 is involved in three of the statistically most representative conformations represented in Fig. 4. In 441, it makes a practically always present HB with Arg4, thus favoring a rather compact conformation by connecting the α-helix and the random coil region.

The question concerning the interaction of the hlF1-11 and control peptides with a membrane can be examined considering the data represented in Fig. 5, where we report the distribution of closest water, methanol and chloroform molecules in the 441 medium (upper row), and of water

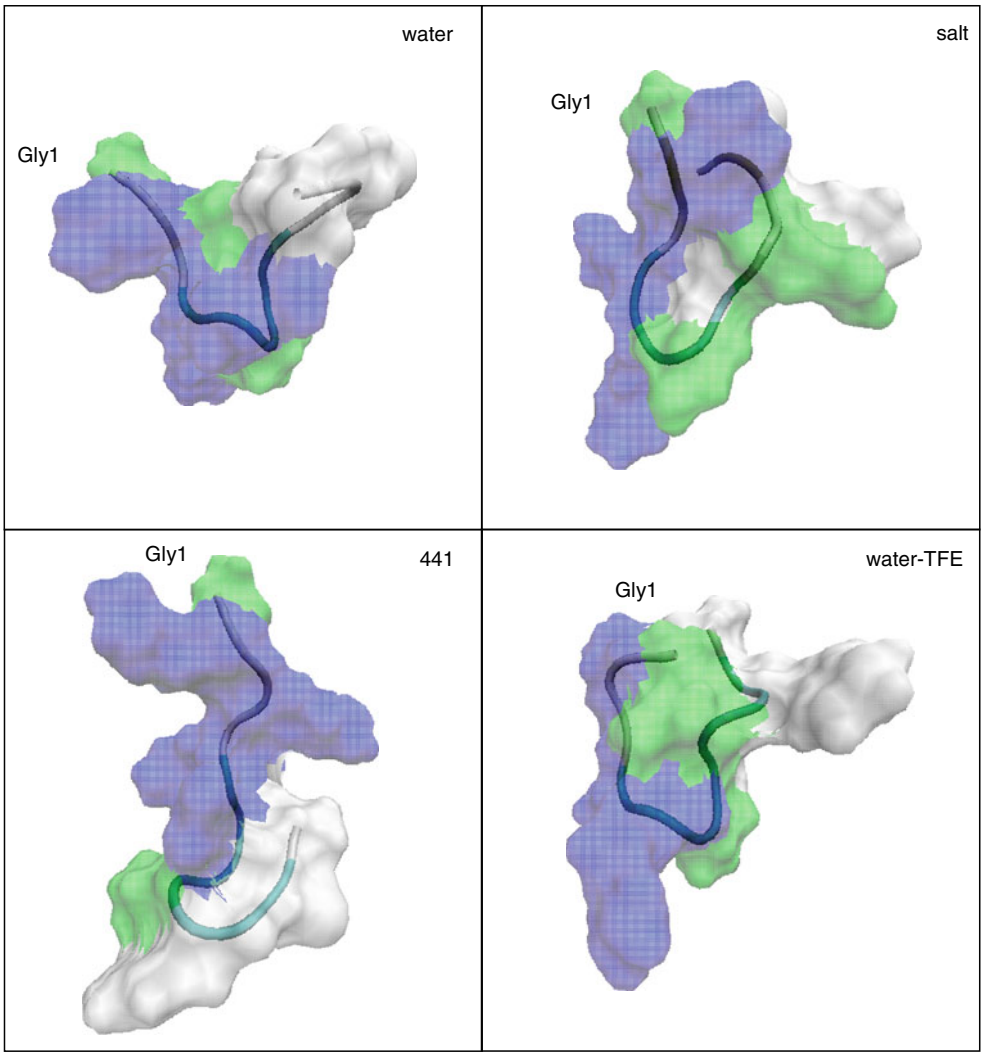

Fig. 3 Molecular surface and backbone visualization of statistically representative conformations of the hlF1-11 most populated clusters evaluated in the 50–100 ns time interval of the simulation in water, 250 mM NaCl, 50% (V/V) water–TFE and 4:4:1 methanol–chloroform–water (clockwise from the top left panel, respectively). Surfaces are drawn with VMD using 1.4-Å probe radius. Color-coding as in Fig. 1

and TFE molecules in the water–TFE mixture (lower row). These results are obtained considering the solvent molecules present within distance of 5.5 Å (namely, the distance corresponding to the first minimum of the radial distribution function of the CCl_4 carbon atoms) from the solute atoms. One can observe that in 441 medium there is a well differentiated distribution of the different types of solvent molecules around the hlF1-11 peptide, whereas it is considerably less so around the control peptide. Indeed, the chloroform molecules surround predominantly the hlF1-11 C-terminal region starting from Ser6 residue, namely the peptide segment constituting the hairpin-shaped loop shown in Fig. 3, suggesting that this peptide segment interacts with the interior of the bacterial membrane (Zhou et al. 2004). After all, this is not unexpected considering the mainly hydrophobic character of this peptide stretch. Instead, the differences in the distribution of the solvent molecules along the control peptide are less relevant, although water and methanol are predominant in the vicinity of Arg4 and Arg5 residues, while chloroform is more present around Val7 and Gln8 amino acids.

In the water–TFE medium, the distributions of water and TFE molecules along hlF1-11 are more uniform than in the 441 case. Nevertheless, water molecules somewhat prevail around the peptide cationic region and TFE molecules are slightly more frequent around the hydrophobic region, with a maximum in correspondence of Trp9 residue, as chloroform does in the 441 case. The solvent distributions are even more uniform along the control peptide, though water is somewhat more present around Arg4 and Arg5 and TFE prevails in the more hydrophobic region. This again parallels what occurs in the 441 case.

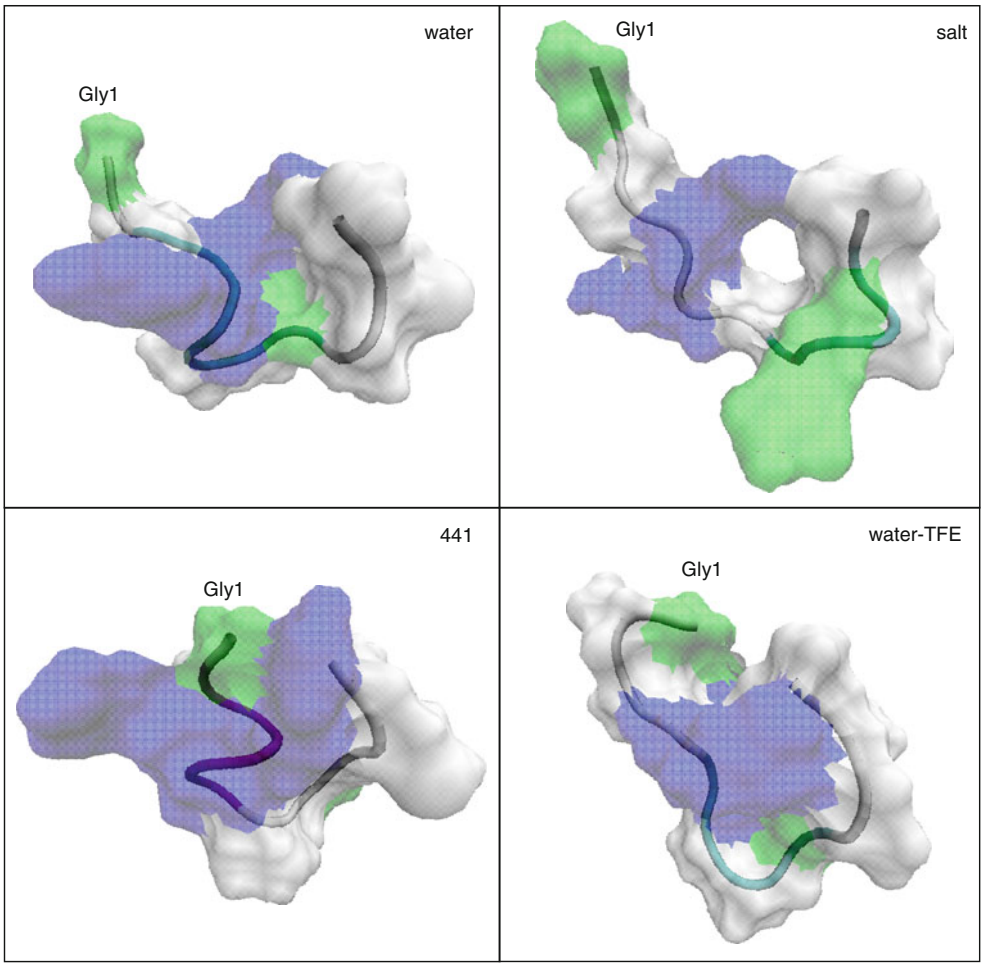

Fig. 4 Same as for Fig. 3 for the control peptide

Table 3 Properties of intramolecular hydrogen bonds (HBs) for hlF1-11 and control peptide in the four solvents considered

	Water	Salt	441	Water–TFE
hlF1-11				
Average HB frequency[a]	17.2	23.9	22.9	49.1
Strongest HB (SHB)	R4:O-V7:HN	W9:O-R3:HN	V7:O-C10:HN	R4:O-V7:HN
Frequency of SHB	98.4	90.0	74.1	99.5
Control				
Average HB frequency[a]	14.6	15.9	38.5	14.3
Strongest HB (SHB)	R4:O-V7:HN	A3:O-Q8:HN	A3:O-Q8:HN	A6:O-Q8:HN
Frequency of SHB	39.1	31.2	97.9	58.7

[a] Considering HBs with frequency ≥5%; HB definition: distance donor–acceptor ≤3.5 Å, donor–H–acceptor angle ≥90°, as in Gangemi et al. (2008)

A more detailed view concerning the solvent effect on the peptide structure is given by Fig. 6 where we report the partial SASA values per residue. As data in Table 2 show, the total SASA values do not change much by varying solvent, the differences with respect to water being within ca. 10%. One can, however, notice that while the hlF1-11 region around Val7 has a low exposition to the solvent in all cases, in 441 the solvent exposition of all polar residues, except Arg5, is notably enhanced. The SASA value of the latter is on the contrary increased in salt and in water–TFE.

The solvent effect on the residue exposition for the control peptide is less readable. The most evident feature is the consistently reduced solvent exposition of Ala residues due to 441, partially related to its helical structure.

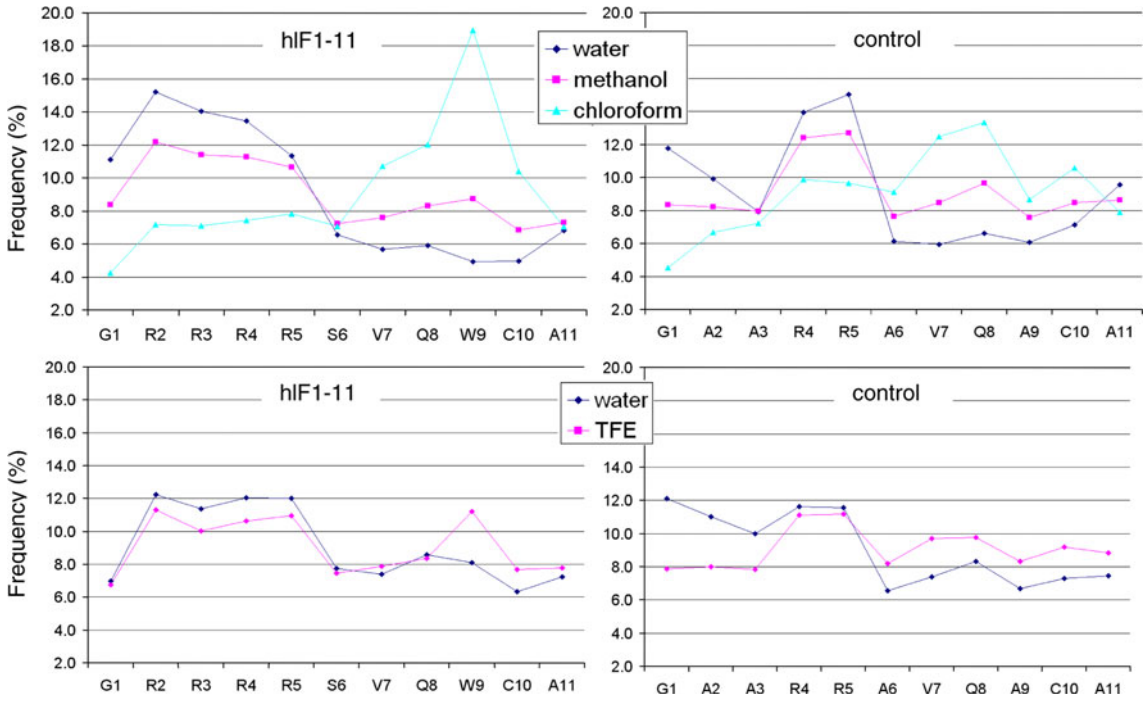

Fig. 5 *Upper row*: percentage distribution of methanol, chloroform and water molecules along hlF1-11 (*left*) and control peptide (*right*) in 441 medium. *Lower row*: percentage distribution of water and TFE molecules along hlF1-11 (*left*) and control peptide (*right*) in water–TFE mixture

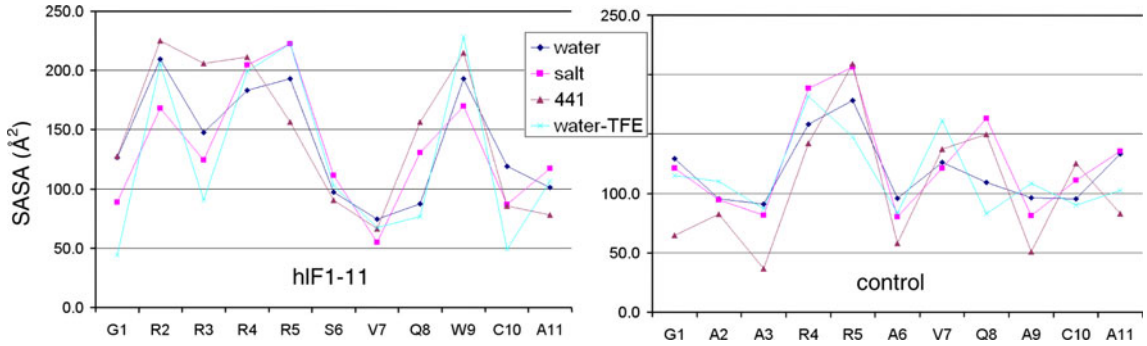

Fig. 6 Solvent accessible surface area (SASA, in Å^2) per residue for hlF1-11 (*left*) and control peptide (*right*), which has been evaluated using a probe radius of 1.4 Å

Some insight into the internal dynamics of hlF1-11 and control peptides in the four solvents is obtained by considering their atomic B-factors, which measure the atomic positional fluctuations. The overall average values for hlF1-11 and control peptide in the four solvents are reported in Table 4. One can see that they are particularly small for hlF1-11 in water–TFE medium and for the control peptide in 441 solvent, paralleling the high degree of the overall hydrogen bonding present in these cases (Table 3).

The B-factor values for each amino acid averaged over the 50–100 ns interval of the trajectories are shown in Fig. 7. We note that they also agree with the previously commented HB features, suggesting that this is the main

Table 4 Average B-factor values (in Å^2) for hlF1-11 and control peptides in the four solvents considered

	Water	Salt	441	Water–TFE
hlF1-11	9.4	7.0	7.0	3.8
Control	12.5	12.0	5.0	6.8

stabilization factor for the peptide conformations. Indeed, the conformations with the lowest positional fluctuations appear to be that of hlF1-11 in water–TFE and that of the control peptide in 441, whose average HB persistence values are 49.1 and 38.5%, respectively (Table 3). Moreover, the regions along both peptides with lower B-factor are often close the strongest HBs. In particular, we see that

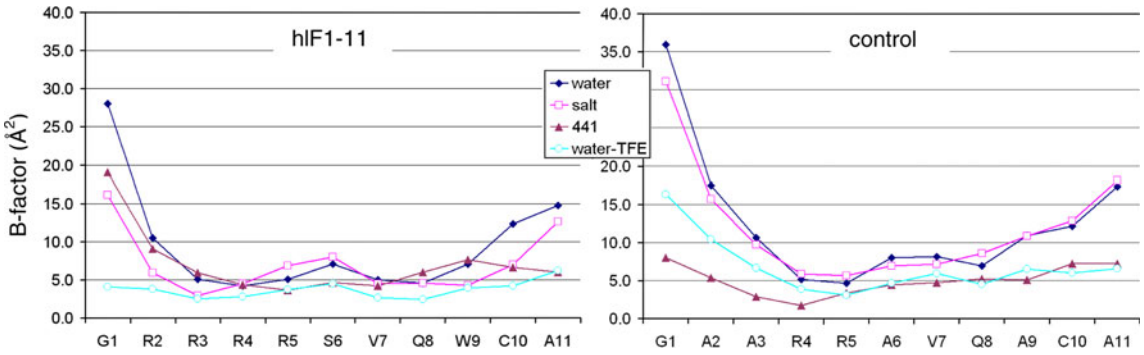

Fig. 7 B-factor values (that is, atomic positional fluctuations, in Å^2) of hlF1-11 (*left*) and control peptide (*right*) backbone atoms of each amino acid for simulations in water, salt, 441 and water–TFE solvents

the hairpin-shaped loop of the hlF1-11 conformation in 441 is stabilized by the HB between Cys10 and Val7, while the mobility of most of its cationic segment is intermediate between those in water and salt cases. We can also observe that the least fluctuating residue is Arg4 of the control peptide in 441, which is in the middle of its α-helix and close to the most persisting HB involving Ala3 and Gln8 residues, as previously noted.

Conclusions

We have performed extensive MD simulations in four different solvents (water, 250 mM NaCl, and membrane-mimicking mixtures 4:4:1 methanol–chloroform–water and 50% (V/V) water–TFE) of the AMP peptide consisting of the first eleven N-terminal amino acids of human lactoferrin (hlF1-11, GRRRRSVQWCA) and of a biologically inactive control peptide (GAARRAVQACA) with Ala substitutions at positions 2, 3, 6 and 9. We can draw the following main conclusions from statistical analyses of the trajectories: (i) in none of the above solvents a hlF1-11 conformation similar to that of the corresponding stretch present in the human lactoferrin protein is statistically predominant; (ii) hlF1-11 only, and particularly in the 441 mixture, presents a structure characterized by an elongated and somewhat mobile cationic region and by a more rigid hairpin-shaped loop in its hydrophobic C-terminal segment. These structural and dynamic differences together with the different distributions of the molecular constituents of the 441 mixture along the peptide suggest that the cationic region is more suitable to optimize its interaction with the membrane anionic polar heads, while the hydrophobic loop—approximately perpendicular to the cationic moiety—can interact with the membrane interior. (iii) The statistically most representative hlF1-11 conformations in 441 and water–TFE solvents are markedly different, although these mixtures are both considered reasonable isotropic mimetics of the membrane environment.

References

Abbate S, Barlati S, Colombi M, Fornili SL, Francescato P, Gangemi F et al (2006) Study of conformational properties of a biologically active peptide of fibronectin by circular dichroism, NMR and molecular dynamics simulation. Phys Chem Chem Phys 8:4668–4677

Allen MP, Tildesley TJ (1987) Computer simulation of liquids. Clarendon Press, Oxford

Bergman DL, Laaksonen L, Laaksonen A (1997) Visualization of solvation structures in liquid mixtures. J Mol Graph Model 15:301–306

Brogden KA (2005) Antimicrobial peptides: pore formers or metabolic inhibitors in bacteria? Nat Rev Microbiol 3:238–250

Brouwer CPJM, Welling MM (2008) Various routes of administration of 99mTc-labeled synthetic lactoferrin antimicrobial peptide hlF1-11 enables monitoring and effective killing of multidrug-resistant Staphylococcus aureus infections in mice. Peptides 29:1109–1117

Caldwell JW, Kollman PA (1995) Structure and properties of neat liquids using nonadditive molecular dynamics: water, methanol and N-methylacetamide. J Phys Chem 99:6208–6219

Case DA, Cheatham TE, Darden T, Gohlke H, Luo R et al (2005) The Amber biomolecular simulation programs. J Comput Chem 26:1668–1688

Case DA, Darden TA, Cheatham TE, Simmerling CL, Wang J, Duke RE et al (2008) AMBER 10. University of California, San Francisco

Chan DIR, Prenner EJ, Vogel HJ (2006) Tryptophan- and arginine-rich antimicrobial peptides: structures and mechanisms of action. Biochim Biophys Acta 1758:1184–1202

Dijkshoorn L, Brouwer CPJM, Bogaards SJP, Nemec A, van den Broek PJ, Nibbering PH (2004) The synthetic N-terminal peptide of human lactoferrin, hLF(1-11), is highly effective against experimental infection caused by multidrug-resistant *Acinetobacter baumannii*. Antimicrob Agents Chemother 48:4919–4921

Fox T, Kollman PA (1998) Application of the RESP methodology in the parametrization of organic solvents. J Phys Chem B 102:8070–8079

Gangemi F, Longhi G, Abbate S, Lebon F, Cordone R, Ghilardi GP, Fornili SL (2008) Molecular dynamics simulation of aqueous solutions of 26-unit segments of p(NIPAAm) and of p(NIPAAm) "doped" with amino acid based comonomers. J Phys Chem B 112:11896–11906

Haney EF, Hunter HN, Matsuzaki K, Vogel HJ (2009) Solution NMR studies of amphibian antimicrobial peptides: linking structure to function? Biochim Biophys Acta 1788:1639–1665

Humphrey W, Dalke A, Schulten K (1996) VMD: visual molecular dynamics. J Mol Graph 14:33–38

Ibragimova GT, Wade RC (1998) Importance of explicit salt ions for protein stability in molecular dynamics simulations. Biophys J 74:2906–2911

Jorgensen WL, Chandrasekhar J, Madura JD, Impey RW, Klein ML (1983) Comparisons of simple potential functions for simulating liquid water. J Chem Phys 79:926–935

Langham AA, Khandelia H, Schuster B, Waring AJ, Leher RI, Kaznessis YN (2008) Correlation between simulated physicochemical properties and hemolycity of protegrin-like antimicrobial peptides: predicting experimental toxicity. Peptides 29:1085–1093

Mottamal M, Shen S, Guembe C, Krilov G (2007) Solvation of transmembrane proteins by isotropic membrane mimetics: a molecular dynamics study. J Phys Chem 111:11285–11296

Nibbering PH, Ravensbergen E, Welling MM, van Berkel L, van Berkel PHC, Pauwels EKJ, Nuijens JH (2001) Human lactoferrin and peptides derived from its N terminus are highly effective against infections with antibiotic-resistant bacteria. Infect Immun 69:1469–1476

Onufriev A, Bashford D, Case DA (2004) Exploring protein native states and large-scale conformational changes with a modified generalized Born model. Proteins 55:383–394

Peterson NA, Arcus VL, Anderson BF, Tweedie JW, Jameson GB, Baker EN (2002) "Dilysine trigger" in transferrins probed by mutagenesis of lactoferrin: crystal structures of the R210G, R210E and R210L mutants of human lactoferrin. Biochemistry 41:14167–14175

Powers J-PS, Hancock REW (2003) The relationship between peptide structure and antibacterial activity. Peptides 24:1681–1691

Ruotolo BT, Russell DH (2004) Gas-phase conformations of proteolytically derived protein fragments: influence of solvent on peptide conformation. J Phys Chem B 108:15321–15331

Shao J, Tanner SW, Thompson N, Cheatam TE (2007) Clustering molecular dynamics trajectories: 1. Characterizing the performance of different clustering algorithms. J Chem Theory Comput 3:2312–2334

Voss NR, Gerstein M (2005) Calculation of standard atomic volumes for RNA and comparison with proteins: RNA is packed more tightly. J Mol Biol 346:477–492

Wang K-R, Zhang B-Z, Zhang W, Yan J-X, Li J, Wang R (2008) Antitumor effects, cell selectivity and structure-activity relationship of a novel antimicrobial peptide polybia-MPI. Peptides 29:963–968

Wickstrom L, Okur A, Simmerling C (2009) Evaluating the performance of the ff99SB force field based on NMR scalar coupling data. Biophys J 97:853–856

Yeaman MR, Yount NY (2003) Mechanisms of antimicrobial peptide action and resistance. Pharmacol Rev 55:27–55

Zhou N, Tieleman DP, Volfel HJ (2004) Molecular dynamics simulations of bovine lactoferrin: turning a helix into a sheet. Biometals 17:217–223